Proposed Fault Detection Algorithm with Optimized Hybrid Speed Control

MARIEM AHMED BABA[1,*], MOHAMED NAOUI[2,*], AHMED ABBOU[1],
MOHAMED CHERKAOUI[1]
[1]Engineering for Smart and Sustainable Systems Research Center,
Mohammadia School of Engineers, Mohammed V University,
BP: 765, Av. Ibn Sina, Agdal - Rabat,
MOROCCO

[2]Research Unit of Energy Processes Environment and Electrical Systems,
National Engineering School of Gabes,
University of Gabés, Gabés 6029,
TUNISIA

**Corresponding Author*

Abstract: - The Brushless DC (BLDC) motor is a common choice for industrial applications, particularly in the automotive sector, owing to its high efficiency and robust capabilities. To detect the position of the motor rotor, hall-effect sensors can be used, but these sensors may prevent the system from operating if they fail. Consequently, fault-tolerant control (FTC) has been proposed in several studies to ensure continuity of operation in the event of sensor failure. This paper proposes an innovative method of fault detection in the hall effect sensor for a BLDC motor using combinatorial functions. This paper proposes an innovative method of hall-effect sensor fault detection for a BLDC motor using combinatorial functions. For the speed control of the BLDC under study, a hybrid adaptive neuro-fuzzy inference control (ANFIS) is implemented. In addition, the FTC signal reconstruction technique adopted has been improved to achieve motor start-up despite a fault in one of the sensors, thanks to well-defined fault detection algorithms. Simulation results are presented for each sensor failure case to test the effectiveness of the method used.

Key-Words: - BLDC motor, Hall position, PID controller, Fuzzy logic controller, fault-tolerant control (FTC); hall effect sensors; artificial neural network (ANN); fuzzy logic (FL); intelligent control; hybrid adaptive neuro-fuzzy inference control (ANFIS).

Received: March 9, 2023. Revised: December 23, 2023. Accepted: March 3, 2024. Published: April 11, 2024.

1 Introduction

Brushless DC (BLDC) motors are widely utilized across various industries including industrial, aerospace, household appliances, and automotive sectors. These motors function similarly to DC motors but without the presence of brushes. They are distinguished by their electronic commutation utilizing semiconductor electronic switches, [1]. The BLDC motor is considered a type of permanent synchronous machine, [2]. The rotor position can be assured by several methods, with or without sensors. In the case of sensors, optical or Hall-effect sensors are used to detect rotor position. The wide use of this motor is due to its considerable advantages, such as high efficiency, low maintenance needs, high torque-to-weight ratio, and low noise, thanks to the absence of brushes, [3]. The automotive sector has introduced the BLDC engine into their models to a considerable extent, [4], [5]. For example, Toyota and Honda, [6], have adopted these engines in models that have become widespread.

In the literature, several papers have discussed applications of the BLDC motor in electric vehicles. For example, in [7], the authors used the regenerative braking technique (RBS) applied to the BLDC motor for electric vehicles. In the same concept, the paper [8], deals with neural network control of an electric vehicle drive train using the brushless motor. In [9], a concrete study is presented to define and discuss the important role of the BLDC motor in promoting the performance of electric vehicles. This work also presented the different controllers widely used in the case of a

BLDC motor, including neural network control and fuzzy logic control.

Other researchers, [10], have adopted the BLDC motor speed control system using the artificial neural network (ANN) controller to apply it to electric buses. As a result, the simulation results obtained in this case demonstrated the effectiveness of the technique employed. In addition, a comparative study of different controllers aimed at controlling a BLDC motor was carried out, [11]. Therefore, the authors proposed several types of control based mainly on adaptive neuro-fuzzy inference systems.

Faults during system operation are a serious concern for vehicle manufacturers, who need to ensure safety and high vehicle performance. Hence, the focus on fault-tolerant control (FTC) is seen as a strategy to ensure that a system continues operating despite faults, [12]. Fault-tolerant control strategies are generally divided into two main groups: active tolerant control and passive tolerant control. In the case of electric vehicle failures, faults can be located either in the actuators or in the sensors. However, many studies have treated the Hall sensor faults as one of the most famous failures. Indeed, the algorithms adopted in FTCs have recently been widely used to improve the system's capabilities, especially in industrial sectors where a small defect in a product can affect its sales. Paper [13], discussed an improved fault tolerant control (FTC) method using a vector tracking observer. This technique improved steady-state and transient operating conditions despite the existence of hall-effect sensor failures. As much research is based on FTC control in the case of a single sensor failure, the authors in [14] propose an innovative method using fault-tolerant direct redundant control to limit the failure effect in the case of multiple sensor failures. Among the methods developed by the FTC, is a technique adopting electronic logic gates that aims to track the state of Hall effect signals to translate them into binary language. Another innovative FTC technique has been applied in [15], using three main indices to detect reversal faults in a brushless motor and another index to identify faulty cases from normal ones. Despite the excessive use of common FTC methods such as fault recovery techniques and the vector tracking observer, it has been observed that the system becomes less flexible when used with different models. To avoid this problem, the authors in [16] presented a new method based on (CNN-LSTM) applied to a BLDC motor for fault detection and signal reconstruction of hall-effect sensors. The authors in [17] proposed a hybrid approach between the genetic and binary state transition algorithms to detect defective BLDC motor bearings. In a comparative study, the Adaptive Neuro Fuzzy Inference System controller (ANFIS) was used to study the speed behavior of a brushless DC motor, [18]. The results in this case showed that the speed obtained by the ANFIS controller was the closest to the reference speed compared with other controllers applied. This hybrid control has also been used in medical applications, [19]. The process serves to improve the speed performance of the BLDC motor using (the ANFIS) controller to apply this strategy to surgical robotic systems. This paper is organized as follows. An overview of the BLDC motor is presented, together with the overall mathematical modeling of this motor. The second section studies the speed control system used. The remaining part uses the binary function method to deal with the hall-effect sensor fault detection strategy. The final section presents simulation results and a discussion of each case.

2 Mathematical Modeling of the Hybrid Vehicle

2.1 Mechanical Model

The mechanical model of a moving vehicle, as shown in Figure 1, is determined by all the forces acting on the direction of motion. To calculate the power necessary for the vehicle to move forward (Pm), we apply the fundamental principle of dynamics (F.P.D):

$$M_v \frac{d\vec{v}}{dt} = \sum \vec{F}\, ext \tag{1}$$

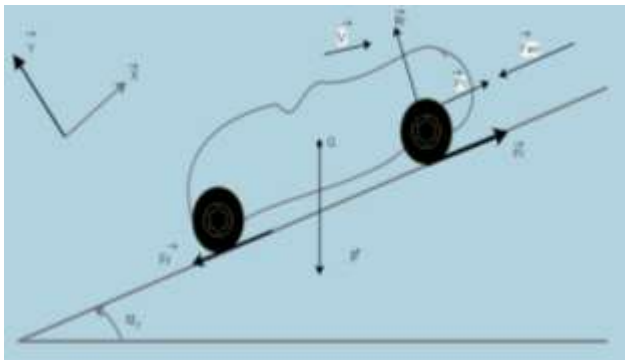

Fig. 1: Balance of forces acting on the vehicle

The balance of external forces is summarized in Figure 1.

$$M_v \frac{d\vec{v}}{dt} = \vec{F}air + \vec{P} + \overrightarrow{Fr} + \overrightarrow{Ft} \tag{2}$$

Where $\vec{F}air$ represents the air resistance on the vehicle, $\overrightarrow{Fr}$ the wheel resistance, and the mechanical traction force:

$$\vec{F}_{air} = -\frac{1}{2}\rho_{air} v^2 S\ C_x\ \vec{x} \quad (3)$$

$$\vec{F}_r = -PR_c\ \cos\alpha_r\ \vec{x} \quad (4)$$

The projection of equation (2) onto the $\vec{x}$ axis:

$$M_v \frac{dv}{dt}\overrightarrow{x} = (-\frac{1}{2}\rho_{air} v^2 S\ C_x - M_v\ g\ \sin\alpha_r - M_v\ g\ R_c\ \cos\alpha_r + F_t)\vec{x} \quad (5)$$

$$F_t = M_v \frac{dv}{dt} + \frac{1}{2}\rho_{air} v^2 S\ C_x + M_v\ g\ \sin\alpha_r + M_v\ g\ R_c\ \cos\alpha_r \quad (6)$$

The mechanical power P_m necessary for the advancement of the vehicle can be expressed through equation (7).

$$P_m = F_t . v \quad (7)$$

Based on equation (5) it is therefore possible to express the mechanical power as in equation (8).

$$P_m = v(M_v \frac{dv}{dt} + \frac{1}{2}\rho_{air} v^2 S\ C_x + M_v\ g\ \sin\alpha_r + M_v\ g\ R_c\ \cos\alpha_r) \quad (8)$$

2.2 Modeling of the Electric Traction System

2.2.1 BLDC Motor Description

The threat of pollution caused by conventional vehicles has prompted the world to use electric vehicles as an alternative. The brushless DC motor (BLDC) is one of the motors most widely used in the drive train of EVs, and has been adopted by several car manufacturers, including Toyota and Honda, [20]. These motors are characterized by an electronic commutation system, which makes them different from DC motors. There are several techniques for determining switching times in electronic switching, the most common of which is Hall-effect sensors. The BLDC motor structure does not contain commutators or brushes and is characterized by a rotating permanent magnet located on the rotor, as well as other magnets attached to the motor housing. The main components of this motor are the stator, composed of concentrated windings, and the rotor, which comes in different types depending on the performance required. The reason for introducing BLDC motors in EVs is their exceptional performance, which includes high efficiency, small size, silent operation, and high power density, [21]. The efficiency of the BLDC motor is considered among the highest in comparison with other types of motor, and it also has a long service life when subjected to normal conditions. On the other hand, this motor is available at a high cost, especially as its system requires electronic control, increasing the total price of the motor and equipment system. This engine has other disadvantages, such as sensitivity to high temperatures, which can indirectly reduce torque, [22]. The control study of a BLDC motor first requires concrete mathematical modeling of the machine. The following section focuses on the mathematical equations of the overall system adopted.

2.2.2 Mathematical Model of a Brushless DC Motor

Modeling a BLDC motor requires the representation of all the electrical and mechanical equations.

A. Electric model

Mathematical motor modeling presents fundamental values such as voltages, currents, and speed. The equations below examine the three-phase winding voltages:

$$\begin{cases} V_a = RI_a + L\left(\frac{di_a}{dt}\right) + e_a \\ V_b = RI_b + L\left(\frac{di_b}{dt}\right) + e_b \\ V_c = RI_c + L\left(\frac{di_c}{dt}\right) + e_c \end{cases} \quad (9)$$

Equations (2), and (3) respectively represent the voltage vector in the 3 phases and the corresponding speed form.

$$\begin{cases} \begin{bmatrix} V_a \\ V_b \\ V_c \end{bmatrix} = \begin{bmatrix} R & 0 & 0 \\ 0 & R & 0 \\ 0 & 0 & R \end{bmatrix} \begin{bmatrix} i_a \\ i_b \\ i_c \end{bmatrix} + \frac{d}{dt} \begin{bmatrix} L_{aa} & L_{ab} & L_{ac} \\ L_{ba} & L_{bb} & L_{bc} \\ L_{ca} & L_{cb} & L_{cc} \end{bmatrix} \begin{bmatrix} i_a \\ i_b \\ i_c \end{bmatrix} + \begin{bmatrix} e_a \\ e_b \\ e_c \end{bmatrix} \quad (10) \\ \mathrm{W} = \frac{\mathrm{d}\theta}{\mathrm{dt}} = \mathrm{p}\frac{\mathrm{d}\theta_\mathrm{r}}{\mathrm{dt}} = \mathrm{pw_r} \quad (11) \end{cases}$$

By using the relationship between electromotive force (EMF) and rotational speed, we obtain the expression for EMF in the form:

$$\begin{cases} e_a = k_e w_r f_a(\theta) \\ e_b = k_e w_r f_b(\theta) \\ e_c = k_e w_r f_c(\theta) \end{cases} \quad (12)$$

The EMF equation is written as follows, where ke is defined by the coefficient of the electromotive force.

$$\begin{cases} e_a = k_e w f(\theta_e) \\ e_b = k_e w f(\theta_e - 2\Pi/3) \\ e_c = k_e w f(\theta_e + 2\Pi/3) \end{cases} \quad (13)$$

The form of the currents is represented by the equations below:

$$\begin{cases} \frac{di_a}{dt} = \frac{1}{3Lm}(2V_{ab} + V_{bc} - 3Ri_a + \Omega PK(-2e_a + e_b + e_c)) \\ \frac{di_b}{dt} = \frac{1}{3Lm}(-V_{ab} + V_{bc} - 3Ri_b + \Omega PK(e_a - 2e_b + e_c)) \\ \frac{di_c}{dt} = -(\frac{di_a}{dt} + \frac{di_b}{dt}) \end{cases} \quad (14)$$

Where (Vab, Vbc) are the corresponding phase-to-phase voltages and Ω represents the mechanical rotational speed.

The motor studied is powered by a three-phase inverter. The inverter part was realized from the following equations:

$$\begin{cases} \mathrm{V_a} = \frac{(\mathrm{S_1})\mathrm{V_d}}{2} - \frac{(\mathrm{S_4})\mathrm{V_d}}{2} \\ \mathrm{V_b} = \frac{(\mathrm{S_3})\mathrm{V_d}}{2} - \frac{(\mathrm{S_6})\mathrm{V_d}}{2} \\ \mathrm{V_c} = \frac{(\mathrm{S_5})\mathrm{V_d}}{2} - \frac{(\mathrm{S_2})\mathrm{V_d}}{2} \end{cases} \quad (15)$$

B. Mechanical system of the BLDC motor

The rotor system of this motor type is generally made of permanent magnet steel with several poles determined according to each series. The following system of equations shows respectively the mechanical equation of motion in (8) and the second equation defining electromagnetic torque (9):

$$\begin{cases} J\frac{d\Omega}{dt} = C_e - f\Omega - C_r & (8) \\ C_e = \frac{P_e}{\Omega} & (9) \end{cases},$$

Ω: Mechanical rotation speed and J represent the moment of inertia

From equation (8) we can also obtain the speed expression.

With Pe Represents electromagnetic power which is expressed as follows:

$$P_e = e_a i_a + e_b i_b + e_c i_c \quad (10)$$

The electromagnetic torque is defined as:

$$C_e = P(e_a i_a + e_b i_c + e_c i_c) \quad (11)$$

P: number of pairs of poles

2.3 Speed Control Techniques for BLDC Motors

The BLDC motor is classified into two types according to the structure of the electromotive force (EMF), whether sinusoidal or trapezoidal. This fem shape results from the interconnection of the coils in the stator windings and also the pole structure of the rotor magnets, [23]. There are several strategies for controlling the speed of a BLDC motor, including sensor-based control, sensorless control, and digital control. In this work, the control method adopted is based on hall-effect sensors. Despite the development of control tools, traditional controllers such as Proportional Integral (PI) and Proportional Integral Derivative (PID) are still included in the list of commonly used controllers. In addition, several systems are based on robust controls such as sliding mode control, [24] and others are based on artificial intelligence such as fuzzy logic control and Adaptive Neuro Fuzzy Inference System controller (ANFIS), [25]. The following section describes the different controllers used in this study.

2.3.1 PI Controller

The PI controller is present in various industrial applications due to its ability to improve motor speed. This controller type consists of correcting the actual speed to approach or reach the desired speed. Its architecture is simple and can be easily implemented, [26].

The controller (PI) is available in several forms, depending on whether it is connected in series or parallel. It is generally presented by the following transfer function:

$$PI(S) = K_P.\frac{w_i}{s}.(1 + \frac{s}{w_i}) \quad (12)$$

Where $w_i = \frac{k_1}{k_2} = \frac{1}{T_i}$.

Kp: proportional gain

*Ki:*integral gain

2.3.2 PID Controller

The block diagram in Figure 2 show the PID (Proportional, Integral, and Deferential) controller is used to control and improve motor speed. In the case of BLDC motor speed control, it offers excellent performance thanks to its reliable and stable system. The proportional action reduces the error, while the integral term pushes the output value to the same value as the setpoint. Derivative action ensures the prediction of potential future errors.

To optimize the adjustment of this controller, several adjustment methods are applied, including Zigler-Nichols, Modulus Optimum, and Åström-Hägglund methods.

The following transfer function is expressed as follows:

$$C(S) = K_p + \frac{K_I}{S} + K_d S \quad (13)$$

The transfer function expression can be written in a simpler way: $C(S) = (K_p S + K_I + K_d S^2)/S$ (14)

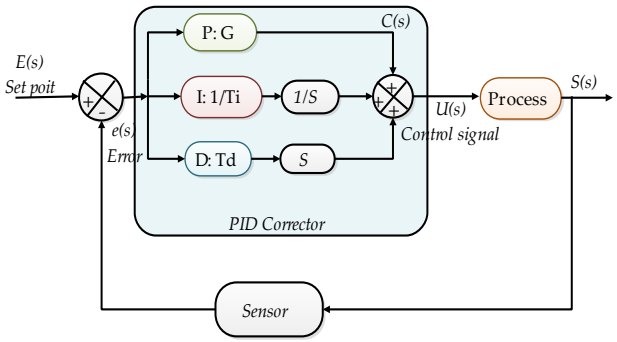

Fig. 2: Block diagram of a PID controller

2.3.3 Fuzzy Logic Controller

Fuzzy logic is derived from artificial intelligence and used primarily to establish control systems that imitate the human mind. The use of fuzzy logic (FL) controllers in non-linear systems continues to grow due to their advantages, including flexibility and robustness. The FL controller also ensures plant non-linearity management without the use of mathematical models. This type of controller is characterized by linguistic terms generally expressed as logical implications based on the "if" and "then" rules, [27]. To create and configure a fuzzy logic controller, the following four phases must be followed:

a. Fuzzification: This operation transforms measured variables into fuzzy linguistic variables using membership functions.
b. Fuzzy Inference: This step determines the control rules needed to obtain the desired results.
c. Defuzzification: It converts all fuzzy output variables into the required net values.

The performance of the fuzzy logic controller can be improved by hybridizing other controllers with it, such as PID-Fuzzy logic and the Adaptive Neuro-Fuzzy Inference System controllers. As indicated in Table 1, the entire set of 49 rules was justified after a thorough series of evaluations.

Table 1. Fuzzy Rule Look-Up Table

E/CE	***NB***	***NM***	***NS***	***Z***	***PS***	***PM***	***PB***
NB	NB	NB	NB	NB	NM	NS	Z
NM	NB	NB	NB	NM	NS	Z	PS
NS	NB	NB	NM	NS	Z	PS	PM
Z	NB	NM	NS	Z	PS	PM	PB
PS	NM	NS	Z	PS	PM	PB	PB
PM	NS	Z	PS	PM	PB	PB	PB

NB: negative big; NM: negative medium; NS: negative small; Z: zero; PS: positive small; PM: positive medium; PB: positive big.

2.3.4 Neuronal Networks Controller

In the field of artificial intelligence, the neural network (ANN) is considered one of the most recommended controllers. Its principle is to simulate the behavior of a biological neural network, such as the human one. This controller has been widely used in BLDC motors for various roles, depending on the desired objective, such as speed estimation or control, [28], [29]. The neural network system essentially comprises four parts: the layer, the neurons, the weights, and the transfer functions.

The neural system depends on several main criteria: the connection indicating the input-output direction, and the weights of the relations, [30]. To obtain the data needed to train the controller (ANN), we first need to store the reference neural network model and then apply it to the electrical system under study.

2.3.5 ANFIS Controller

The ANFIS (Adaptive Neuro Fuzzy Inference System) controller is considered to be a combination of artificial neural networks and fuzzy logic in the form of a well-defined algorithm. This control technique has become very popular recently, thanks to its performance features such as the simplicity of its learning algorithms, [31] and the improved robustness of the system. The structure of the ANFIS controller consists of a network of linked nodes with inputs and outputs that depend on the learning system implemented to achieve the desired goal of error minimization. The structure of the ANFIS controller consists of a network of linked nodes with inputs and outputs that depend on the learning system implemented to achieve the desired goal of error minimization. The system of this controller is based on four blocks which are respectfully fuzzification, knowledge base, neural network, and defuzzification. Consequently, the adopted fuzzy inference set has two inputs (x,y) and one output z.

In the case of ANFIS controllers, the error is expressed as follows:

$$e = S_r - S_a \quad (15)$$

Where S_r represents the desired speed and S_a represents the actual rotor speed. Despite the ANFIS controller being used to control speed, it has also been used in other innovative areas. For example, in [32], a comparative study was carried out to test the predictive ability of student performance, using both hierarchical ANFIS and ANN systems, and the results showed the success of the hierarchical ANFIS model.

3 Proposed Hybrid Speed Control

The proposed system consists of applying hybrid control (ANFIS) to a BLDC motor.

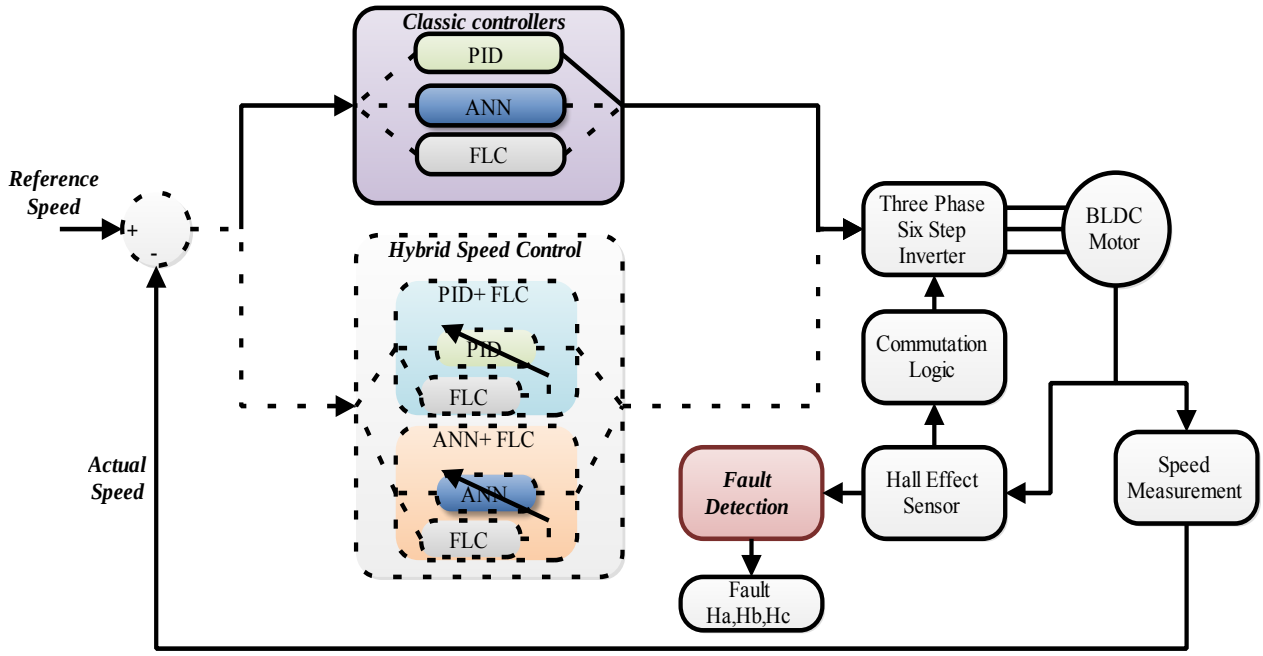

Fig. 3: Block of control system applied and Fault detection control

The control is realized by combining the fuzzy logic controller and the neural network controller. After determining the mathematical modeling of the motor, a control study is carried out to produce a single robust control system that combines the performance of the two proposed controllers. The second part of this work consists in studying the fault of the hall effect sensors implemented. Therefore, a fault-tolerant control was presented to ensure system operation in the presence of faults. Figure 3 shows the system studied for speed control of a BLDC motor, with the different control techniques applied. This diagram shows the general structure of the system as it operates during simulation in the MATLAB simulink environment. It also includes a dedicated fault detection phase for hall-effect sensors.

3.1 Proposed Fault Detection

The three hall-effect sensor signals (Ha, Hb, and Hc) vary according to the rotor position of a BLDC motor. These sensors provide six sequences for 360°, a process that results from phase current switching according to the chosen direction of rotor rotation. When a fault occurs, the six sectors supplied by the three Habc signals become four sectors only. This implies that there are two erroneous commutations in two sectors, and the phase is switched off in the case of the third sector as show Figure 4.

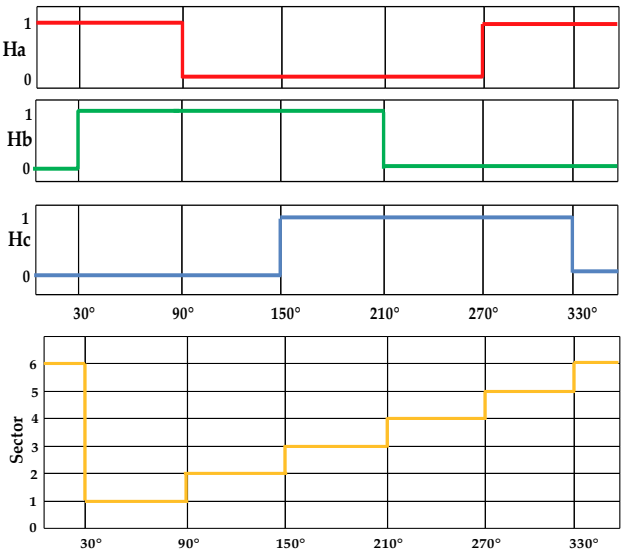

Fig. 4: Normal operation (a) Hall signals. (b) Sector

3.2 The Strategy Adopted for Sector Reconstruction

For BLDC motor control, a performance algorithm is proposed to ensure correct operation if one or both sensors fail. As a precautionary measure, three circuits are available for signal reconstruction. In the event of a sensor fault, one of these circuits

reconstructs the sectors to ensure continuity of operation.

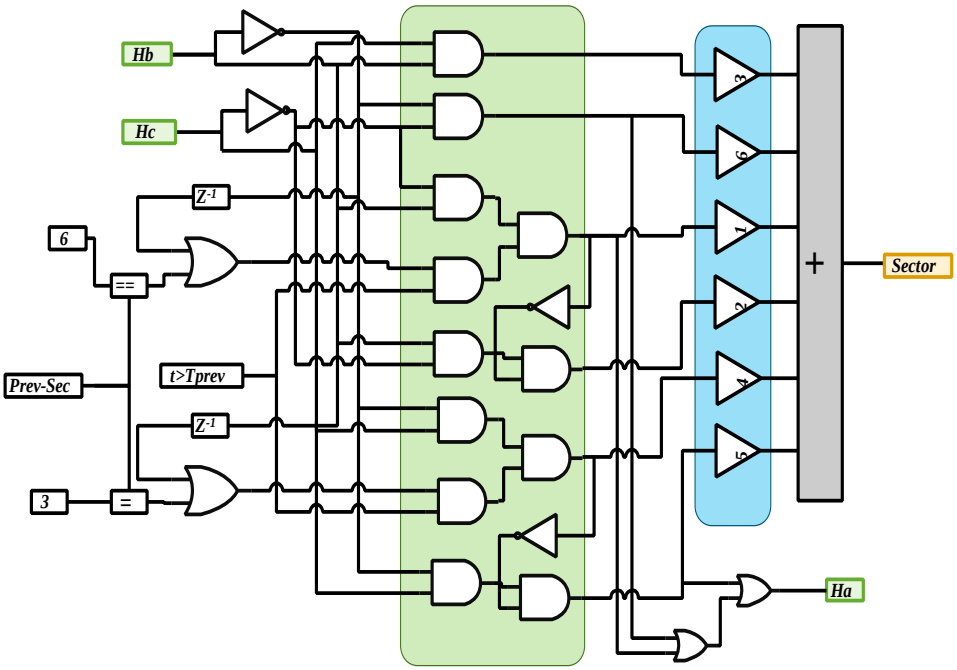

Fig. 5: Proposed scheme for reconstructing the signal if Ha is faulty

In addition, a system for improving the algorithm used to reconstruct sectors has been applied during engine start-up. This initiative guarantees safe starting in the event of sensor faults. This technique enables the reconstruction algorithm to distinguish between sectors 1 and 2, and also between sectors 4 and 5.

If the BLDC motor rotates counter-clockwise, the following circuit is obtained: sector 1 → sector 2 → sector 3 → sector 4 → sector 5 → sector 6. As the case studied consists of faulty Hall-effect sensors, the sectors supplied become four instead of the six sectors in the normal state. Therefore, the Ha sensor is considered faulty if it persists in providing a value of 1 or 0.

As a result, the scenarios presented in the case of sensor fault Ha are summarized in Figure 5, where the proposed signal reconstruction method ensures immediate fault detection.

4 Simulation Results

The results obtained from simulation in MATLAB Simulink are based on a BLDC control system using the following controllers: PI, PID, neural network, fuzzy logic, and hybrid control (ANFIS). This simulation aims to test the fault detection strategy applied to hall-effect sensors and to discuss the efficiency of the algorithm that ensures sector reconstruction. The results presented consist of observing the following parameters: Rotor speed with and without fault, the signals from the three sensors (Ha, Hb, and Hc), the sectors constructed by the proposed algorithm, and the corresponding currents.

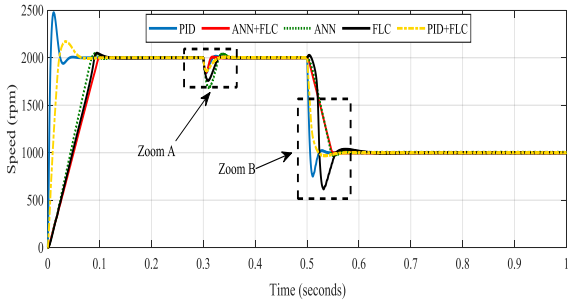

(a)

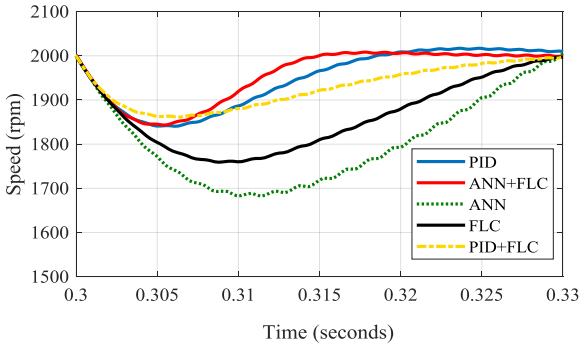

Zoom A

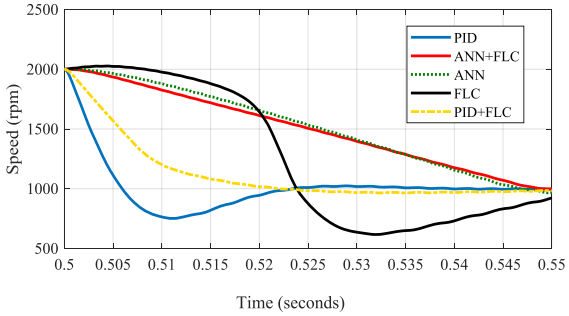

Zoom B

(b)

Fig. 6: Rotor speed of the BLDC motor according to controllers applied (PID, FLC, ANN, ANFIS) in case of faults. (**a**): speed, (**b**) Zoom A, B

Figure 6 shows the different states of Speed in each case for the controllers used. It can be seen that the ANFIS or (ANN+FLC) controller shows a delay at start-up, but in particular, has the most stable curve, with a minimum peak compared with the other controllers, which is equal to the instant t=0.3s, as shown in Figure ZOOM A. Consequently, Figure ZOOM B shows the disturbed phase at time t=0.5s where the ANFIS controller curve gives the fastest speed response.

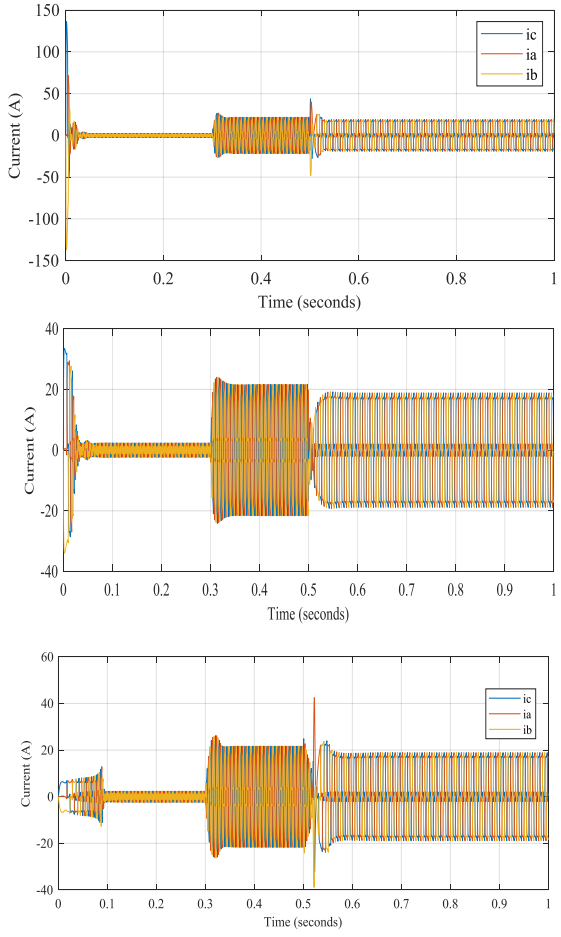

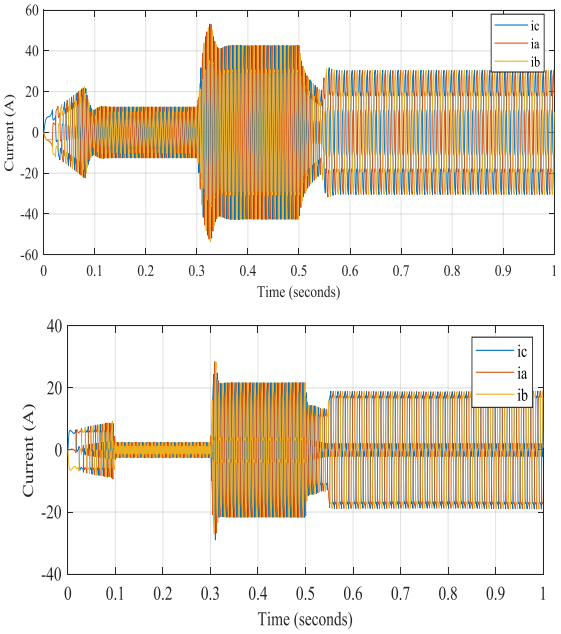

Fig. 7: Structure of currents in each type of controller applied (PID, FLC, (PID+FLC) ANN, and ANFIS)

Figure 7 shows the different forms of phase current using five controllers. The current curve for neural network control showed limited disturbance, but the current curve for hybrid ANFIS control was the best, providing the most stable current.

Table 2 compares various operating characteristics such as rising time, settling time, and overshoot percentage.

Table 2. Speed response characteristics

Controller	***Rise time (sec)***	***Settling time (sec)***	***Overshoot Percentage (%)***
PID controller	*0.03*	*0.06*	*40*
ANN controller	*0.01*	*0.03*	*84*
FLC+PID	*0.06*	*0.054*	*87*
ANN+FLC	*0.012*	*0.023*	*98*

5 Fault Tolerance Detection

This section discusses the failure states of the H_a, H_b, and H_c sensors, and the results show the signal reconstruction in each case.

Case 1: faults located in the H_a sensor

The Ha sensor fault occurs at t=0.7s in Figure 8 when Ha goes from 0 to 1. The sector then changes after the fault and takes on a new phase between [0,4] instead of the normal phase between [1,6].

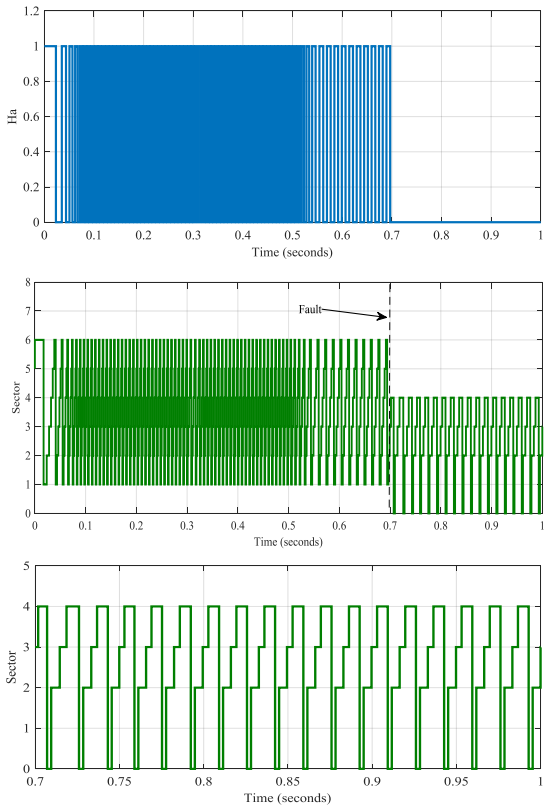

Fig. 8: H_a sensor results in the presence of a fault

Case 2: faults located in the H_b sensor
The H_b sensor fault occurs at t=0.7s as shown in Figure 9, when Ha goes from 0 to 1. The sector then changes after the fault and takes on a new phase between [0,6] instead of the normal phase between [1,6].

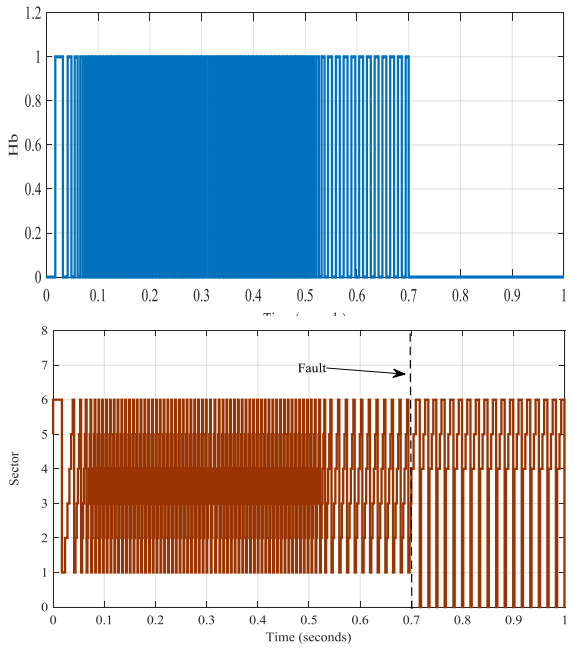

Fig. 9: H_b sensor results in the presence of a fault

Case 3: faults located in the HC sensor
The H_c sensor fault occurs at t=0.7s as shown in Figure 10, when Ha goes from 0 to 1. The sector then changes after the fault and goes from [0,6] to [6,1] instead of the normal phase between [1,6].

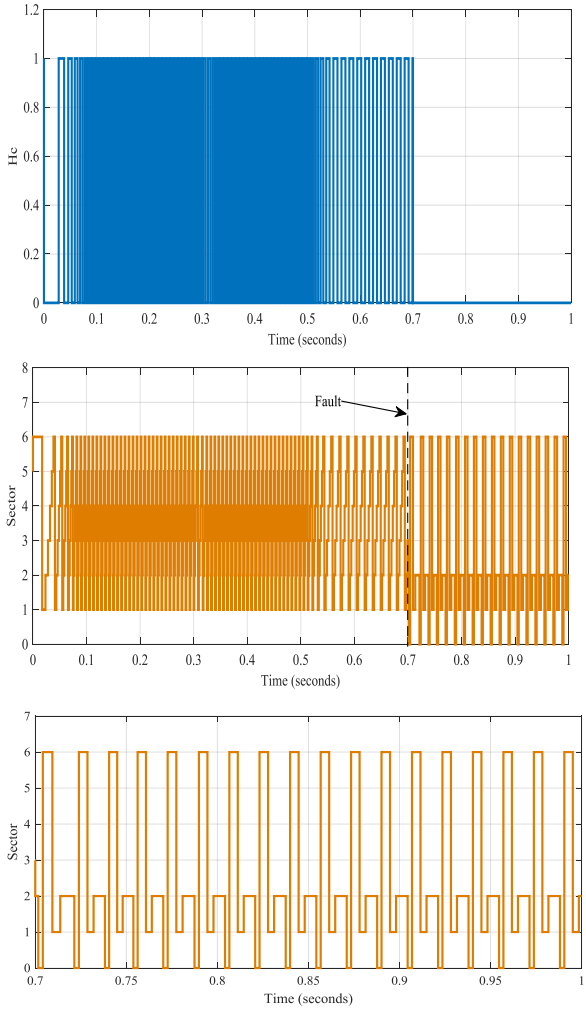

Fig. 10: H_c sensor results in the presence of a fault

Case 4: Two or more faults Sensor
A problem with two or more malfunctions in the BLDC motor sensor that results in the system stopping or failing. In extreme cases, persistent sensor malfunctions may lead to system shutdown or complete motor failure. This can result in downtime and the need for extensive troubleshooting and repairs. Addressing sensor malfunctions promptly through proper diagnostics and troubleshooting is crucial to restoring the reliable and efficient operation of BLDC motors.

6 Conclusion

This paper examines a developed fault detection strategy adopted for a BLDC motor intended for

electric vehicles. A study on speed control of the BLDC motor was conducted using an ANFIS hybrid controller, which yielded significant results compared to other controllers. The fault detection technique is applied to hall-effect sensors to identify faults and ensure uninterrupted system operation. This study examines both single-sensor fault and dual-sensor fault scenarios, demonstrating the effectiveness of the proposed method in maintaining system functionality. In our future work, building upon previous projects, we will introduce an enhanced method for detecting and rectifying faults in Ha, Hb, and Hc sensors using sector reconstruction techniques. Additionally, we aim to develop a detection strategy for mechanical or electrical faults such as short circuits and winding failures.

Acknowledgement:
This paper was completed thanks to the fellowship the Organisation for Women in Science for the Developing World (OWSD) and the Swedish International Development Cooperation Agency (SIDA) provided. The author would like to express her warmest thanks for the support that contributed to the success of this article.

References:

[1] Alsayid, B., Salah, W. A., & Alawneh, Y. (2019). Modeling of censored speed control of BLDC motor using MATLAB/SIMULINK. *International Journal of Electrical and Computer Engineering*, *9*(5), 3333.

[2] Singh, B., & Singh, S. (2009). State-of-art on permanent magnet brushless DC motor drives. *Journal of power electronics*, *9*(1), 1-17.

[3] Boldyriev, S., Steshenko, T., Serohina, S., Fomina, S., & Kapelista, I. (2024). Exercise of State Control over Local Self-Government in the Field of Environmental Protection. *WSEAS Transactions on Environment and Development*, *20*, 26-36, DOI: 10.37394/232015.2024.20.4.

[4] Godfrey, A. J., & Sankaranarayanan, V. (2018). A new electric braking system with energy regeneration for a BLDC motor-driven electric vehicle. *Engineering Science and Technology, an international journal*, *21*(4), 704-713, https://doi.org/10.1016/j.jestch.2018.05.003.

[5] Minh, D. B., Quoc, V. D., & Huy, P. N. (2021). Efficiency Improvement of Permanent Magnet BLDC Motors for Electric Vehicles. *Engineering, Technology & Applied Science Research*, *11*(5), 7615-7618.

[6] Bhatt, P., Mehar, H., & Sahajwani, M. (2019). Electrical motors for electric vehicle–a comparative study. *Proceedings of Recent Advances in Interdisciplinary Trends in Engineering & Applications (RAITEA)*.

[7] Nian, X., Peng, F., & Zhang, H. (2014). Regenerative braking system of electric vehicle driven by brushless DC motor. *IEEE Transactions on Industrial Electronics*, *61*(10), 5798-5808, https://doi.org/10.1109/TIE.2014.2300059.

[8] Kanchev, H., Hinov, N., Gilev, B., & Francois, B. (2018). Modelling and control by neural network of electric vehicle traction system. *Elektronika ir* Elektrotechnika, 24(3), 23-28, https://doi.org/10.5755/j01.eie.24.3.20974.

[9] Song, Z., Fan, X., & Gan, J. (2018). Review on control of permanent magnet brushless DC motor for electric vehicle. *International Journal of Electric and Hybrid Vehicles*, *10*(4), 347-365, https://doi.org/10.1504/IJEHV.2018.098121.

[10] Pamuji, F. A., Prihantari, K. J., Riawan, D. C., Asfani, D. A., Suryoatmojo, H., Guntur, H. L., & Arumsari, N. (2022). Application of Artificial Neural Network for Speed Control of BLDC Motor 90KW in Electrical Bus. *Przeglad Elektrotechniczny*, *98*(2). DOI: 10.15199/48.2022.02.47.

[11] Intidam, A., El Fadil, H., Housny, H., El Idrissi, Z., Lassioui, A., Nady, S., & Jabal Laafou, A. (2023). Development and Experimental Implementation of Optimized PI-ANFIS Controller for Speed Control of a Brushless DC Motor in Fuel Cell Electric Vehicles. *Energies*, *16*(11), 4395, https://doi.org/10.3390/en16114395.

[12] Sunthornwat, Rapin, Yupaporn Areepong, and Saowanit Sukparungsee. "Performance Evaluation of HWMA Control Chart based on AR (p) with Trend Model to Detect Shift Process Mean." *WSEAS Transactions on Business and Economics*, 21 (2024): 603-616, https://doi.org/10.37394/23207.2024.21.50.

[13] Dong, L., Huang, Y., Jatskevich, J., & Liu, J. (2016). Improved fault-tolerant control for brushless permanent magnet motor drives with defective hall sensors. *IEEE*

Transactions on Energy Conversion, *31*(2), 789-799.

[14] Aqil, M., & Hur, J. (2021). Multiple sensor fault detection algorithm for fault tolerant control of BLDC motor. *Electronics*, *10*(9), 1038, https://doi.org/10.3390/electronics10091038.

[15] Jafari, A., Faiz, J., & Jarrahi, M. A. (2020). A simple and efficient current-based method for interturn fault detection in BLDC motors. *IEEE Transactions on Industrial Informatics*, *17*(4), 2707-2715, DOI: 10.1109/TII.2020.3009867 .

[16] Chu, Kenny Sau . K., Chew, Kuew . W., & Chang, Yoong. C. (2023). Fault-Diagnosis and Fault-Recovery System of Hall Sensors in Brushless DC Motor Based on Neural Networks. *Sensors*, *23*(9), 4330, https://doi.org/10.3390/s23094330.

[17] Yauri, Ricardo, Santiago Fernandez, and Anyela Aquino. "Control of Autonomous Aerial Vehicles to Transport a Medical Supplies." WSEAS Transactions on Systems 23 (2024): 73-81. DOI: 10.37394/23202.2024.23.8.

[18] Suryoatmojo, H., Pratomo, D. R., Soedibyo, M. R., Riawan, D. C., Setijadi, E., & Mardiyanto, R. (2020). Robust speed control of brushless dc motor based on adaptive neuro fuzzy inference system for electric motorcycle application. *International Journal of Innovative Computing Information and Control*, *16*(2), 415-428. DOI: 10.24507/ijicic.16.02.415.

[19] Gandhi, Shreya. U., & Prasad, B. Swathi. (2020). Modelling and intelligent control of micro PMBLDC for surgical robotic applications. *Procedia Computer Science*, *171*, 745-754, https://doi.org/10.1016/j.procs.2020.04.081.

[20] Koten, H., & Bilal, S. (2018). Recent developments in electric vehicles. *Intern J Adv Autom Technol*, *1*(1), 35-52, http://dx.doi.org/10.15659/ijaat.18.01.890.

[21] Khluabwannarat, P., Nawikavatan, A., & Puangdownreong, D. (2018). Fractional-order model parameter identification of BLDC motor by flower pollination algorithm. *WSEAS Transactions on Systems and Control*, *13*, 573-579.

[22] Yildirim, Merve., Polat, Mehmet., & Kürüm, H. (2014, September). A survey on comparison of electric motor types and drives used for electric vehicles. In *2014 16th International Power Electronics and Motion Control Conference and Exposition* (pp. 218-223), Antalya, Turkey, IEEE. https://doi.org/10.1109/EPEPEMC.2014.6980715.

[23] Popenda, A. (2018). Modelling of BLDC motor energized by different converter systems. *Przegląd Elektrotechniczny*, *94*, 81-84. doi:10.15199/48.2018.01.21.

[24] Chan, Jun Wei. (2022). Sliding Mode Control of Brushless DC Motor Speed Control. *Malaysian Journal of Science and Advanced Technology*, 188-193, https://doi.org/10.56532/mjsat.v2i4.57.

[25] Intidam, A., El Fadil, H., Housny, H., El Idrissi, Z., Lassioui, A., Nady, S., & Jabal Laafou, A. (2023). Development and Experimental Implementation of Optimized PI-ANFIS Controller for Speed Control of a Brushless DC Motor in Fuel Cell Electric Vehicles. *Energies*, *16*(11), 4395.

[26] Yilmaz, U., Kircay, A., & Borekci, S. (2018). PV system fuzzy logic MPPT method and PI control as a charge controller. *Renewable and Sustainable Energy Reviews*, *81*, 994-1001, https://doi.org/10.1016/j.rser.2017.08.048.

[27] Voynarenko, M. P., Dzhedzhula, V. V., Hurochkina, V. V., Yepifanova, I. Y., & Menchynska, O. L. E. N. A. (2021). Applying fuzzy logic to modeling economic emergence. *WSEAS Transactions on Business and Economics.* Vol. 18: 424-434, https://doi.org/10.37394/23207.2021.18.43.

[28] Unlersen, M. Fahri., Balci, S., Aslan, M. F., & Sabanci, K. (2022). The speed estimation via BiLSTM-based network of a BLDC motor drive for fan applications. *Arabian Journal for Science and Engineering*, *47*(3), 2639-2648.

[29] Rif'an, M., Yusivar, F., & Kusumoputro, B. (2019). Sensorless-BLDC motor speed control with ensemble Kalman filter and neural network. *Journal of Mechatronics, Electrical Power, and Vehicular Technology*, *10*(1), 1-6, https://doi.org/10.14203/j.mev.2019.v10.1-6.

[30] Solanki, Sakshi. (2016). Brushless DC motor drive during speed regulation with artificial neural network controller. *International Journal of Engineering Research and Applications*, *6*(6), 01-05.

[31] Kiani Mavi, R., Kiani Mavi, N., & Goh, M. (2017). Modeling corporate entrepreneurship success with ANFIS. *Operational Research*, *17*, 213-238.

[32] Do, Quang.H., & Chen, Jeng-Fung. (2013). A comparative study of hierarchical ANFIS and ANN in predicting student academic

performance. *WSEAS Transactions on Information Science and Applications*, 12(10), 396-405.

Contribution of Individual Authors to the Creation of a Scientific Article (Ghostwriting Policy)

The authors equally contributed to the present research, at all stages from the formulation of the problem to the final findings and solution.

Sources of Funding for Research Presented in a Scientific Article or Scientific Article Itself

No funding was received for conducting this study.

Conflict of Interest

The authors have no conflicts of interest to declare.